

Original article

**INHIBITORY EFFECT OF PLANTS EXTRACT AGAINST THE FUNGAL GROWTH ON THE ARCHAEOLOGICAL SANDSTONES IN TELL-BASTA OPEN AREA**

Elnaggar, M.<sup>1(\*)</sup>, Ghally, M.<sup>2</sup>, Adam, M.<sup>3</sup> & Mansour, M.<sup>3</sup>

<sup>1</sup>Conservation dept., General Administration of Restoration of Antiquities and Museums of East Delta, Ministry of Tourism & Antiquities, Sharkia, Egypt

<sup>2</sup>Bot. Microbiology dept., Faculty of science, Zagazig Univ., Zagazig, Egypt

<sup>3</sup>Conservation dept., Faculty of Archaeology, Cairo Univ., Cairo, Egypt

\*E-mail address: [mennamaher1989@gmail.com](mailto:mennamaher1989@gmail.com)

**Article info.**

**Article history:**

Received: 24-8-2023

Accepted: 18-2-2024

Doi: 10.21608/ejars.2024.396684

**Keywords:**

Tell Basta

Sandstone

Biodeterioration

Fungal growth

Plant extract

Clove

Garlic

EJARS – Vol. 14 (2) – Dec. 2024: 181-190

**Abstract:**

Fungi play a very important role in the biodegradation of archaeological stones in Tell Basta open area, leading to their biodeterioration and loss. Therefore, it was necessary to preserve these archaeological stones, especially sandstone. The sandstone was analyzed and examined using X-ray diffraction (XRD), X-ray fluorescence (XRF) and scanning electron microscopy (SEM) for deteriorated fungal growth and compared with control. Deteriorated fungi isolated from sandstone, such as *Curvularia. spp.*, *A. niger*, *A. flavus*, and *A. terreus* and their deterioration were studied. Plant extracts have been used to inhibit fungal growth because they are ecofriendly materials, harmless to the restorer, and economically inexpensive. This study presents a new method for inhibiting fungal growth on the surface of sandstone located at an open site in Egypt, using plant extracts. Fungal growth was inhibited using different concentrations of aqueous garlic extract (900 µg/µl, 630 µg/µl, 360 µg/µl, 180 µg/µl) and methanolic clove extract (500 µg/µl, 375 µg/µl, 250 µg/µl, 125 µg/µl). Measuring the MFC value of the aqueous extract of the garlic plant and the methanolic extract of the cloves to determine the lowest concentration showed no visible fungal growth, and detecting the purified active components against deteriorated fungal growth of cloves.

**1. Introduction**

The ancient Egyptian city of Tell Basta (Bubastis) located in the southern Nile delta in the city of Zagazig, the provincial seat Sharkiya, of considered an important archaeological site. It was inhabited from the Predynastic Era (late 4<sup>th</sup> millennium BC) until Roman domination [1,2]. Sedimentary rocks such as sandstone are composed primarily of small rock fragments or mineral particles. Quartz often forms sandstones. Feldspar is another component in sandstone, which includes both K feldspar and Na or Ca feldspar. Sandstone can also contain other minerals such as mica, clay minerals, lithic fragments, and accessory minerals [3-5]. Many investigations have been conducted to better understand the factors contributing to stone deterioration, including chemical, physical, and microbial growth [6]. Most geology textbooks categorize weathering into two categories: physical weathering, which includes fires, frost action, insolation, salt weathering as a result of crystallization and hydration pressures, and plant root action; and chemical weathering, which includes the dissolution of certain stony minerals, oxidation, and hydrolysis [7]. Acidic rain penetrates the stone, causing internal pressure, cracks, and crusts

[8]. This process alters minerals through dissolution, oxidation, and other chemical reactions, and when minerals disintegrate, some elements leach out, leading to a change in the geochemistry [9]. On the other hand, biodeterioration processes in stone decay are greatly influenced by water availability and environmental conditions. Anthropogenic pollutants can serve as nutrient demands for stone-colonizing microorganisms [10]. Additionally, it was discovered that microorganism can growth on sandstone and penetrate the pores, producing acids that make color change. The microbes grow on rock surfaces are called 'epilithic'. Additionally, microbes that are in the pore space of sandstone are called 'endolithic' and can cause cracks and alteration to rocks [11]. Also, microbes can damage the surface of stones through biofilm formation, chemical reactions with the substrate, physical penetration into the substrate, and pigment production. However, the colonization of stones by microbes depends on environmental factors such as water availability, pH, exposure to the external climate, and nutrient sources [6,12]. Generally microbial biodeterioration involves the metabolic production of organic and inorganic

acids. This acid degradation is one of the most well-known biogeochemical mechanisms of rock disintegration [13]. In temperate or humid conditions, hyphomycetes (mold) produce mycelium in the porous spaces of the stones [14]. Moreover, some species of the genus *Aspergillus* and *Curvularia* cause various colors and organic acids, can cause dissolution of mineral components and the rock binder, leading to crusting of the stone material. This was clearly observed on the surface of sandstone [15]. Also, the fungus produces colored spots on rock surfaces such as *A. niger* and *A. flavus* produce oxalic acid, citric acid, gluconic acid, fumaric acid, and succinic acid. Furthermore, *Curvularia lunata* produces oxalic acid and *A. terreus* produces acids with melanin [16-19]. Stone discoloration is usually caused by microbial pigments, in which their metabolites may lead to aesthetic damage as well as physical damage by producing acids as a result of fungal activity and growth [20-22]. Plant extracts have been used to reduce biological damage. The phytochemical investigation of neem, moringa, jatropha, and balanites crude leaf extracts revealed bioactive plant components with potential antimicrobial properties. The highest activity was found in the methanol extract when compared to the ethanolic and aqueous extracts [23,24]. All fungi's growth was completely inhibited for a variety of times up to 21 days when crushed cloves (*Eugenia caryophyllus*) and garlic (*Allium sativum*) were added to potato dextrose agar. Clove was the strongest antifungal plant [25]. Extraction of plant components is frequently done using a number of techniques, including sonification, heating under reflux, Soxhlet extraction, and others, are frequently used. Additionally, fresh green plants or dried powdered plant material are soaked in distilled water or organic solvent systems, then the plant is filtered to create plant extracts and stored at a low temperature in darkness until use. The applicability of the extraction techniques must be taken into account, as the plant components may range from non-polar to polar and may be affected by thermal pressure for a long time [24,26]. The aim of this work was to assess the deterioration caused by the fungi that can colonize sandstone in the Tell Pasta area, by examining sandstone and control of the isolated fungi with ecofriendly materials and evaluate effect of plant extract when applied on the sandstone surface in this condition.

## 2. Material and methods

### 2.1. Sampling

In April 2021, samples were collected to investigate fungi by swabbing surfaces with sterile cotton swabs. The samples were obtained from different spots of the change of color sandstone located in the open-area museum in Tal Basta area within the city of Zagazig, Sharkia Governorate, fig. (1) [27].



Figure (1) swabs places from the sandstone surface (Samples B1: B6)

## 2.2. Investigation and analyses methods

### 2.2.1. Polarized light microscope (PLM)

Thin sections of sandstone samples were studied to identify the nature of the mineral components and deterioration manifestations, using light polarized microscope (PLM) (Gippon Japan (Inc.)) in the geology dept., Faculty of Science, Zagazig Univ. Thin sections, cut across the thickness of the stone, were used to determine the different typologies of sandstone [6,28].

### 2.2.2. Scanning electronic microscope (SEM)

SEM evaluation the infected and standard (control) samples of stone were evaluated using scanning electron microscope analysis SEM (Quanta FEG250, with tungsten electron source, at 20 kV). Moreover, EDX was used for elemental analysis.

### 2.2.3. X-ray diffraction analysis (XRD)

Sandstone samples were analyzed to identify their constituent elements using X-ray fluorescence by model 7602EA A1melo Manufactured by Panalytical B.V Co., Netherlands (ISO 9001/14001 KEMA – 0.75160) from Housing and Building National Research Center [6,28].

## 2.3. Isolation, purification and Identification

Samples were obtained by using a wet sterile cotton swab for laboratory testing from the surface of biodegraded sandstone at Tell Basta that showed signs of the biodegradation process, such as discoloration (most often blackening) and surface structure alterations [15]. The swabs were transferred to the microbial laboratory Zagazig Univ. The samples were grown on PDA (potato dextrose agar) (200g Potato extract, 20g Agar and 20 g dextrose) plates and incubated for 7 days at  $25 \pm 2$  °C [6,15]. The single fungal colony was purified several times to obtain a pure fungal colony. The resulting cultures were purified and the isolated fungal culture was studied. The macroscopic characteristics of colonies growing on agar plates were used to identify fungi, as well as the color, size, and morphology structures [29]. Fungi were examined and identified morphologically under a light microscope (Tension, USA) in the Microbiology dept., Faculty of Science - Zagazig Univ.

## 2.4. Fungal colonization test

Sandstone was cut into cubes with a size of  $1 \times 1 \times 1$  cm for samples and autoclaved at a temperature of  $121^\circ\text{C}$  and pressure of 1.5 lb, followed by 24 hours of drying at  $105^\circ\text{C}$  in an oven. For the inoculation of spore suspensions, each cultivated fungal pure colony (7-day-old) on culture plates containing PDA was cultivated with 10 ml of potato broth media (potato 50 g, dextrose 50 g, and distilled water 1L). Spores were discharged using a sterilized needle in an aseptic condition and then the shaking tube was prepared for use [6,30]. To analyze the stone blocks before and after infection, fungal species were purposefully injected into stone cubes. The cubes were placed in sterile glass petri plates, cleaned in an incubator,

and cultured for eight months at 30°C before assessing the colonization [6,19,30]. The fungal growth developed on the stone's surface was examined by Labored light microscope in the Geology dept., Faculty of Science, Zagazig Univ., Then, samples was examined by a Philips XL 30 ESEM in NRC in Dokky, Cairo, Egypt, to identify fungal growth on the biodegradation stone's surface. The elemental analysis and characterization of the stone sample was described by using ESEM coupled with electron dispersive X-ray spectroscopy (EDX). The deteriorating samples before (control) and after inoculation were examined using EDX analysis to show changes in surface morphology and particle size [6, 31,28].

### 2.5. Anti-fungal activities of plant extracts

Plant extracts were prepared by soaking the grinding plant in cold water, boiling water, and methanol. Plants (*clove, garlic, cinnamon, ginger, rosemary, aloe vera, neem, ocimum, lantana, alcanfor, and cymbopogon*) were collected, grinding to fine particles, and then dried in airtight containers at room temperature. One gram of plant was placed into a flask and 10 ml of distilled water or methanol was added to cover the plant. The plant was then boiled with distilled water for 20 minutes. The contents were kept in an orbital shaker for 48 hours on a hot plate magnetic stirrer to stir the extract well. The extract was then filtered through a Whatman No. 1 filter paper and dried in a hot air oven at 40°C for 3 hours to remove excess solvent. Then kept at 4°C for further use [23, 26,32]. It has been noted that the clove plant extract is a colored extract, so it was necessary to remove this color in order to not change the appearance of the archaeological sandstone. This was done by using activated carbon charcoal for the clove plant extract at an amount of 1 g/l. This amount can be increased if needed, fig. (2) [33]. Spectrophotometers device (model UV-3101PC, from National Institute of Metrology and Calibration - Al Haram - Giza - Egypt) (CIE-Commission Int. d'Éclairage) was used for measuring the amount of color change on sandstone samples after treating them with aqueous garlic extract and methanolic clove extract, after removing the color with activated charcoal and comparison with a control sample.

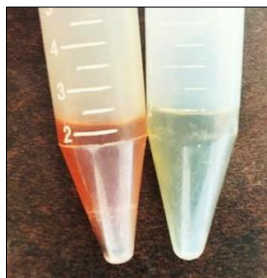


Figure (2) remove color of clove extract using activated charcoal

#### 2.5.1. Determination of the minimum inhibition concentration (MIC) and the minimum fungicidal concentration (MFC).

To confirm the MIC value for each tested fungus, several concentrations of the plant extract were prepared using a microdilution measurement in triplicate, in addition to the original concentration [34]. To examine the inhibitory effect

of the highest selected agents (garlic and cloves) on fungal growth [32]. The following concentrations of methanolic clove extract (500 µg/µl, 375 µg/µl, 250 µg/µl, 125 µg/µl, 62.5 µg/µl), and aqueous garlic (900 µg/µl, 630 µg/µl, 360 µg/µl, 180 µg/µl, 90 µg/µl), were used against different types of fungi. The MIC was determined to measure the plant extracts' antifungal properties quantitatively [35]. The MIC values were selected as the lowest antimicrobial concentration that completely inhibited fungal growth. The lowest concentration, which was characterized as the MFC, showed no visible growth after sub-culturing on fresh medium [36,37].

#### 2.5.2. Preparation of antimicrobial activity disc

Sterile filter paper disc was inserted into 20-40 mL of garlic and clove extracts using a micropipette after Whatman's No. 1 filter paper was punched into 5 mm disc form and sterilized. Small equal amounts of the condensed extracts were put on the discs, and they were then left to dry in the aseptic air. After that, they may be kept at 40°C until use [23]. Sterile PDA was added to sterile petri dishes, and after the liquid had solidified, fresh fungal cultures were swabbed onto the plates. Using sterile forceps, antimicrobial activity discs (sterile discs containing plant extract) were held over the agar plates at different concentrations. The plates were incubated for 24 hours at 27°C. After incubation period, the diameter of the inhibition zones that formed around each disc was measured in (mm) and recorded [23].

#### 2.5.3. Evaluation of active compounds for effective extract using GC-MS

The chemical composition of plant-purified samples was performed using a Trace GC-TSQ mass spectrometer (Thermo Scientific, Austin, TX, USA) (Atomic Energy Authority, Cairo, Egypt). The components were identified by comparing their mass spectra with those of the WILEY 09 and NIST 14 mass spectral databases [38].

## 3. Results

### 3.1. Isolation and identification by light microscope

Forty swabs were taken from the surface of biodegraded sandstone. These swabs were colonized in 40 petri dishes containing PDA media. The swabs showed many types of fungi. Fourteen fungal species belonging to five genera were visually examined and identified morphologically under a light microscope. The percentage distribution of fungal species in inoculated Petri dishes was determined per plate, tab. (1).

Table (1) the distribution percentage of isolate fungi %

NO	Fungi	NO. of fungal per plate	The distribution percentage %
1	<i>Aspergillus niger</i>	38	95%
2	<i>Aspergillus flavus</i>	36	90%
3	<i>Aspergillus terreus</i>	32	80%
4	<i>Curvularia. spp</i>	28	70%
5	<i>Fusarium poae</i>	18	45%
6	<i>Aspergillus parasiticus</i>	18	45%
7	<i>Penicillium chrysogenum</i>	16	40%
8	<i>Aspergillus versicolor</i>	10	25%
9	<i>Aspergillus restrictus</i>	11	27.5%
10	<i>Emericella nidulans</i>	7	17.5%
11	<i>Aspergillus clavatus</i>	5	12.5%
12	<i>Aspergillus fumigatus</i>	3	7.5%

Fungal distribution percentage showed that *A. niger* appeared in 95%, *A. flavus* appeared in 90%, *A. terreus* appeared in 80%, *Curvularia* appeared in 70%, *Fusarium poae* appeared in 45%, *A. parasiticus* appeared in 45%, *P. chrysogenum* appeared in 40%, *A. versicolor* appeared in 25%, *A. restrictus* appeared in 27.5%, *Emericella nidulans* appeared in 17.5%, *A. clavatus* appeared in 12.5% and *A. fumigatus* appeared in 7.5% of petri dishes containing PDA media which colonized by swabs. Many fungi have been photographed under the light microscope, so to examine and visually identify their type according to the shape conidiophore and hyphae of fungi, fig. (3).

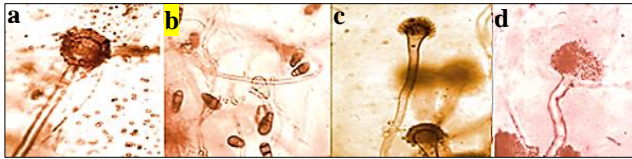


**Figure (3)** hyphal and sporangiophore of fungi under light microscope; **a.** *A. niger*, **b.** *Curvularia* sp., **c.** *A. fumigatus*, **d.** *A. terreus*.

### 3.2. Microscopic examination of stone

#### 3.2.1. Polarized light microscope (PLM)

The studied sandstone samples represent the quartz arenite. Quartz arenite is a type of sandstone consisting of quartz granules with a ratio greater than 90% and a ratio of clay minerals less than 15%. It tends to be light grey with pink and yellow and some brown color, and that's due to the presence of iron oxides, fig. (4-a). The microscopic examination of sandstone samples under PLM Crossed-Nicoles (CN) revealed the presence of monazite mineral as a result of the mineral transformation of quartz. Moreover, the alteration of K-feldspar into kaolinite and sericite, figs. (4-b, c & d).

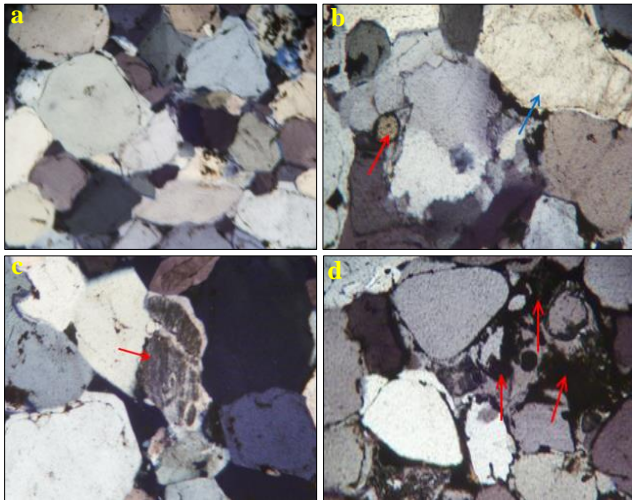


**Figure (4)** PLM photomicrographs of studied sandstone samples shows **a.** the erosion of quartz grains and the weakness and disintegration of the binding material between the quartz grains. Moreover, it shows the presence of iron oxides X-5, **b.** the red arrow indicates to the presence of monazite mineral as a result of the mineral transformation of quartz. The blue arrow indicates to the alteration of potassium feldspar to kaolinite and sericite X-10, **c.** the alteration of potassium feldspar to kaolinite and sericite X-5, **d.** the alteration of potassium feldspar to clay minerals X-5

#### 3.2.2. Scanning Electronic Microscopy (SEM-EDX)

SEM examination shows the morphology of the sandstone surface fig. (5). Moreover, the examination shows the presence

of clay minerals either as a binding material or as a result of the alteration of K-feldspar (Kaolinization) and sodium chloride salt (halite). and the voids between grains due to the loss of the binding materials (granular disintegration). The analysis for the checkpoint of weathered sandstone surface by EDX, tab. (2) showed some elements such as C, O, Na, Mg, Al, Si, Cl, Ca, Ti, K and Fe indicate the existence of salts of halite, alteration into clay minerals fig. (6).

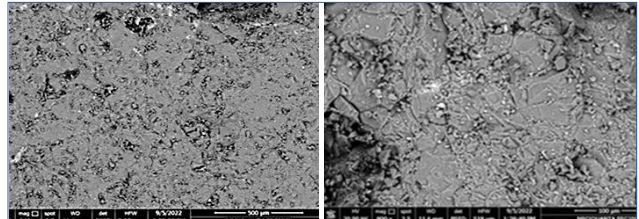


**Figure (5)** SEM photomicrograph of un-colonized (Control) sandstone cubes

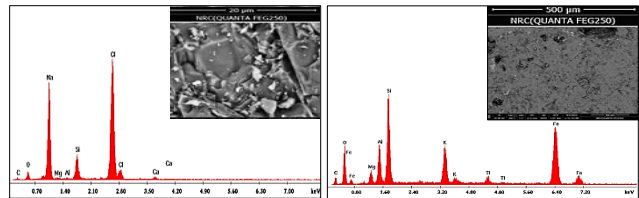


**Figure (6)** EDX analysis of weathered Sandstone surface

**Table (2)** EDX elemental composition of analyzed sample

Samples	Element (Wt. %)										
	C	O	Na	Mg	Al	Si	Cl	K	Ca	Ti	Fe
S 1	8.04	7.92	30.14	0.56	0.40	7.23	44.33	-	1.37	-	-
S 2	12.23	24.39	-	3.35	9.19	18.70	-	7.01	-	1.49	23.63

### 3.3. X-ray analysis of stone

#### 3.3.1. XRD

Analyzed sandstone sample using X-ray diffraction fig. (7) proved that it consists mainly of Quartz, which, indicates that this stone consists of pure quartz (sandstone).

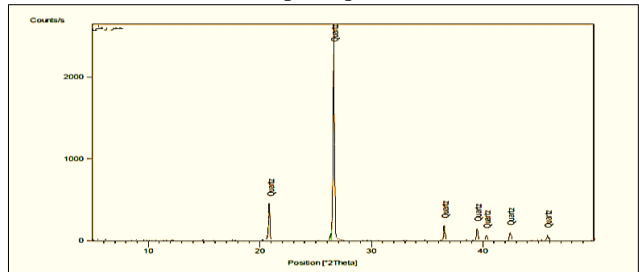


**Figure (7)** XRD pattern of sandstone

#### 3.3.2. XRF

The stone elements analyzed using X-ray fluorescence proved that it consists of a high ratio of silica (Si 94.94%), in addition to other elements such as (Si, Al, Fe, Ca, Mg, Na, K, S, P, Ti, Cr, Zr, Sr, Cl and Lol as listed in tab. (3).

**Table (3)** elements of sandstone analyzed by X-ray fluorescence

Element (Wt. %)															
SiO <sub>2</sub>	Al <sub>2</sub> O <sub>3</sub>	Fe <sub>2</sub> O <sub>3</sub>	CaO	MgO	Na <sub>2</sub> O	K <sub>2</sub> O	SO <sub>3</sub>	P <sub>2</sub> O <sub>5</sub>	TiO <sub>2</sub>	Cr <sub>2</sub> O <sub>3</sub>	ZrO <sub>2</sub>	SrO	Cl	Lol	Total
94.9	0.19	3.04	0.37	0.05	0.03	0.04	0.13	0.06	0.05	0.33	0.32	0.01	0.04	0.38	99.94

### 3.4. Colonization test

Acids and melanin are related to the biochemical characterization of the activity of fungal isolates on sandstones. Most of the fungi species produce acids, while only *Curvularia* and *A. terreus* produced melanin cubes before (control) and after inoculation were examined visually and it was found that

fungi colonized in surface and caused deterioration, discoloration and missed some parts of the stone surface, fig. (8).

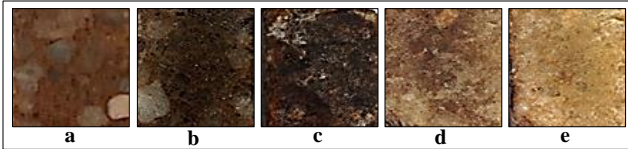


**Figure (8)** **a.** uncolonized sandstone (control) and colonized sandstone by **b.** *A. niger*, **c.** *Curvularia. Spp.*, **d.** *A. terreus*, **e.** *A. flavus*

### 3.5. SEM of colonized and incubated samples

Examination of colonized and incubated cubes shown under SEM, fig. (9) is illustrated and clearly demonstrates the different aspects of deterioration including discoloration, dark pigmentation and stone decay. It is possible to use scanning microscopes for identifying fungus species through the size and shape of their spores, mycelium and hyphae. Many sandstone samples infected with fungi have been examined under the SEM to examine the extent of damage on the surface of the sandstone infected by fungi, such as *Curvularia. Spp.*, *A. terreus.*, *A. flavus.*, and *A. niger*. The fungal mycelium was distributed around the grains. It has been shown that the fungi caused the loss of some minerals, as well as the occurrence of cracks, where hyphae and their roots penetrate the sandstone minerals. Our results, fig. (9-a) show *Curvularia. spp.* It had black colonies, unbranched Conidiophores, brown Conidia, 3-septate, obovoidal. The conidia were fusiform with straight to slightly curved in shape. *Curvularia. spp* causes serious damage to the surface of the sandstone, as we notice large and deep cracks on the surface of the sandstone, in addition to the black discoloration of the sandstone surface. This is because *Curvularia spp* secretes the melanin pigment melanin. Also, fig. (9-b) shows *A. terreus*. The colonies are brown in color with a yellow to deep brown, pyriform vesicles, conidial heads. *A. terreus* causes decay of the surface of the sandstone, as we notice large and deep cracks. In addition, parts of the sandstone surface are lost. This is due to the fact that *A. terreus* dissolves and feeds on some of the components of the sandstone as well as the binding minerals, as it is obvious that the fungus comes out of the missing part. Furthermore, fig. (9-c) shows *A. flavus* conidiophore is a thick-walled branch. The conidiophores are unbranched and are composed of the foot cell, stipe, and vesicle. Conidial heads are light to deep yellow, green, or green. Colonies are granular, flat. Conidia are globose to sub-globose. *A. flavus* causes decay of the surface of sandstone, where we notice the presence of large and small cracks. It is clear that the fungi come out from the cracks after the dissolution of some of the bonding minerals of the surface of the stone. Moreover, fig. (9-d) shows *A. niger* has black spores (conidia) due to its high melanin content. The hyphae of *A. niger* are septate, hyaline and the conidiophores are long, becoming darker at the top and ending in a globose to sub-globose vesicle, tending to split into several loose columns with age. The *A. niger* fungus causes severe deterioration of the sandstone surface, as we observe the decomposition and loss of many parts of the sandstone and the spread of the *A. niger* fungus in the missing parts. This is because the fungi dissolve and feed on most of the components of

sandstone, and therefore *A. niger* is considered one of the most severe fungi that causes severe biodeterioration to sandstone.

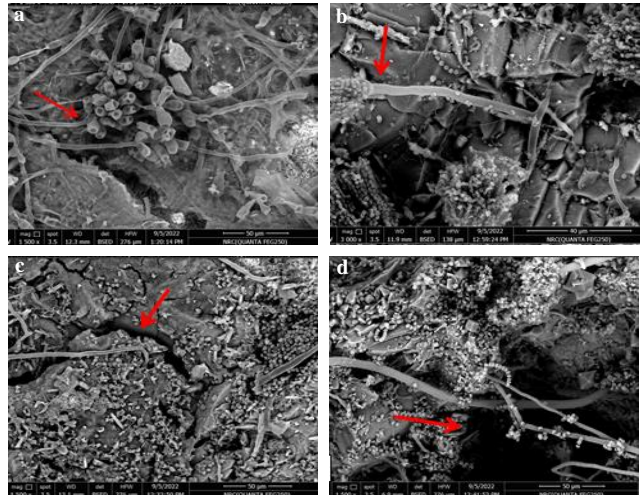


**Figure (9)** SEM photomicrographs of biogenic alteration and the highly fungi-altered affected colonized sandstone samples; **a.** *Curvularia. Spp.*, **b.** *A. terreus*, **c.** *A. flavus*, **d.** *A. niger*.

### 3.6. Antimicrobial screening of plant extracts

The antimicrobial activity of methanol and aqueous extracts of 12 plants were studied using a disc diffusion method against selected fungi inside the PDA media, each dish was divided into two halves, and one extract was applied into each half of the dish to evaluate their effect on the linear growth of fungi. The results obtained showed that there were some plant extracts that reduced the growth of all tested fungi such as clove 500 µg/µl and garlic 900 µg/µl. There are plant extracts that have less effect on fungi such as lemon grass 500 µg/µl, onion 900 µg/µl, cinnamon 500 µg/µl and rosemary 500 µg/µl, but there were plant extracts that had no significant effect on fungal growth such as ginger 500 µg/µl, ocimum 500 µg/µl, aloe vera 900 µg/µl, alcanfor 500 µg/µl, neem 500 µg/µl and lantana 500 µg/µl, fig. (10). The results showed that the best plant extract that showed great effectiveness against most fungi was the methanolic clove extract 500 µg/µl and the aqueous garlic extract 900 µg/µl. Therefore, different concentrations were made from them to determine the value of (MFC).

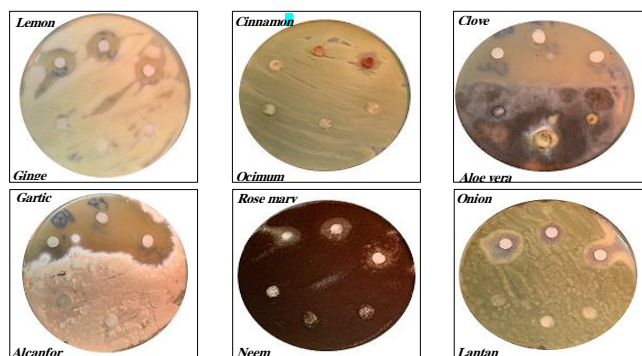


**Figure (10)** the effect of 12 active plant extracts on 6 selected fungal

### 3.7. Value of MIC and MFC of clove and garlic extract

Microdilution measurement (5% conc.) was performed to confirm the MIC value for each fungus tested. Aqueous garlic extract MIC= 180 µg/µl and methanolic clove extract MIC=

125 µg/µl which, showed good antifungal activity with significant inhibition percentage, fig. (11). The MFC was also measured after determining the MIC to determine that the lowest concentration showed no visible growth, as the aqueous garlic extract showed that the MFC in some fungi was at 630 µg/µl such as *Curvularia. spp.*, and the MFC was 360 µg/µl for other fungi such as *A. terreus*, while MFC for methanolic clove extract was 250 µg/µl for all fungi.

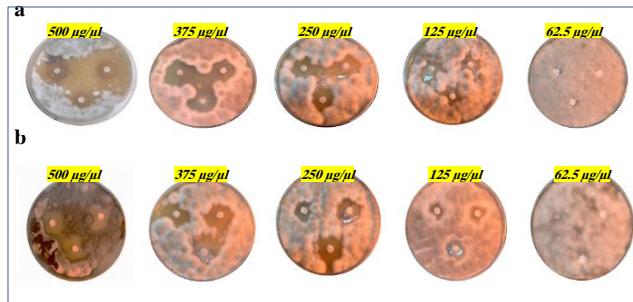


**Figure (11)** MIC of plant extracts on some fungi, **a.** *Curvularia. spp* under the influence of different concentrations of clove, **b.** *Curvularia. spp* under the influence of different concentrations of garlic

The antifungal activity of aqueous garlic extract using disc diffusion method, 180 µg/µl concentration of garlic showed maximum inhibition zone (14.148 mm) against *A. terreus*, (10.852 mm) against *curvularia. spp.*, (5.963 mm) against *A. flavus*, (3.074 mm) against *A. niger*. 360 µg/µl concentration of garlic showed maximum inhibition zone (15.407 mm) against *A. terreus*, (12.815 mm) against *curvularia. spp.*, (9.148 mm) against *A. flavus*, (4.704 mm) against *A. niger*. 630 µg/µl concentration of garlic showed maximum inhibition zone (17.593 mm) against *A. terreus*, (15.185 mm) against *curvularia. spp.*, (10.148 mm) against *A. flavus*, (5.370 mm) against *A. niger*. 900 µg/µl concentration of garlic showed maximum inhibition zone (20.259 mm) against *A. terreus*, (17.889 mm) against *curvularia. spp.*, (11.518 mm) against *A. flavus*, (7.259 mm) against *A. niger* after 48 h, tab. (4). Herein, there were highly significant effects of varying concentrations of aqueous garlic extract on the diameter of inhibition zones for all studied fungi ( $p < 0.0001$ ). A positive correlation was observed, indicating that higher concentrations of the extract resulted in larger inhibition zones, tab. (4). The regression analysis further revealed that the different concentrations of aqueous garlic extract accounted for a substantial portion of the total variation in the inhibition zone diameter. Specifically, the concentrations of aqueous garlic extract explained 92%, 96%, 94%, and 99 % of the total variation in the inhibition zone diameter of *A. Niger*, *A. Terreus*, *A. Flavus*, and *Curvularia. spp.*, respectively, tab. (4). The antifungal activity of methanolic Clove extract using disc diffusion method, 180 µg/µl concentration of clove showed maximum inhibition zone (12.333 mm) against *Curvularia. spp.* (6.259 mm) against *A. niger*, (5.741 mm) against *A. flavus* (5.111mm) against *A. terreus*. 360 µg/µl concentration of cloves showed maximum inhibition zone (16.778 mm) against *Curvularia. spp.* (11.852 mm) against *A. flavus*, (9.111 mm) against *A. terreus* (9.037 mm) against *A. niger*. 630 µg/µl concentration of clove showed maximum-

inhibition zone (19.926 mm) against *Curvularia. spp.* (12.667 mm) against *A. flavus* (11.222 mm) against *A. niger*, (10.741 mm) against *A. terreus*. 900 µg/µl concentration of cloves showed maximum inhibition zone (27.630 mm) against *Curvularia. spp.* (15.296 mm) against *A. flavus*, (14.333 mm) against *A. niger* (11.741 mm) against *A. terreus* after 48 h, tab. (5). The results of this study demonstrated significant effects of methanolic clove extract on the inhibition zones diameter for all tested fungi ( $p < 0.001$ ). The maximum effects were detected at the highest concentration (500 µg/µl), while the lowest doses (125 µg/µl and 250 µg/µl) showed comparatively lower effects ( $p < 0.05$ ), tab. (5). Furthermore, the findings from the linear regression analysis revealed a significant positive relationship between the diameter of inhibition zones and the levels of methanolic clove extract. Specifically, for each unit increase in the concentration of methanolic clove extract, the diameter of inhibition zones increased by 0.108 mm for *A. niger*, 0.088 mm for *A. terreus*, 0.119 mm for *A. flavus*, and 0.201 mm for *curvularia. spp.*, tab. (6).

**Table (4)** effect of different levels from aqueous garlic extract on the inhibition zone diameter (mm) of Fungi

Garlic levels µg/µl	Inhibition zone (mm)			
	<i>A. niger</i>	<i>A. terreus</i>	<i>A. flavus</i>	<i>Curvularia. spp</i>
180	3.074±0.353 <sup>e</sup>	14.148±0.387 <sup>d</sup>	5.963±0.206 <sup>d</sup>	10.852±0.098 <sup>d</sup>
360	4.704±0.161 <sup>b</sup>	15.407±0.370 <sup>c</sup>	9.148±0.161 <sup>c</sup>	12.815±0.289 <sup>c</sup>
630	5.370±0.412 <sup>b</sup>	17.593±0.259 <sup>b</sup>	10.148±0.185 <sup>b</sup>	15.185±0.134 <sup>b</sup>
900	7.259±0.407 <sup>a</sup>	20.259±0.464 <sup>a</sup>	11.518±0.074 <sup>a</sup>	17.889±0.111 <sup>a</sup>
<i>p</i> -value	0.0002	<.0001	<.0001	<.0001

<sup>a,b,c,d</sup> Means in the same column with different superscript letter following them are significantly different ( $p < 0.05$ ).

**Table (4)** regression coefficient of inhibition zone diameter (mm) of fungi on the different levels from aqueous garlic extract

Garlic levels	<i>A. niger</i>	<i>A. terreus</i>	<i>A. flavus</i>	<i>Curvularia. spp</i>
<i>a</i>	2.1340±0.444	12.1736±0.470	5.2221±0.488	8.8396±0.269
<i>b</i> -reg	0.0539±0.007	0.0850±0.007	0.0722±0.007	0.0972±0.004
<i>R</i> <sup>2</sup>	92.00	96.00	94.00	99.00
<i>p</i> -value	<.0001	<.0001	<.0001	<.0001

*a*: intercept; *b*-reg: regression coefficient; *R*<sup>2</sup>: coefficient of determination.

**Table. (5)** Effect of different levels from methanolic clove extract on the inhibition zone diameter (mm) of selected fungi

Clove levels µg/µl	Inhibition zone (mm)			
	<i>A. Niger</i>	<i>A. Terreus</i>	<i>A. Flavus</i>	<i>Curvularia. spp</i>
125	6.259±0.464 <sup>d</sup>	5.111±0.064 <sup>e</sup>	5.741±0.134 <sup>e</sup>	12.333±0.390 <sup>d</sup>
250	9.037±0.303 <sup>c</sup>	9.111±0.577 <sup>b</sup>	11.852±0.582 <sup>b</sup>	16.778±0.588 <sup>c</sup>
375	11.222±0.231 <sup>b</sup>	10.741±0.243 <sup>ab</sup>	12.667±0.339 <sup>b</sup>	19.926±0.901 <sup>b</sup>
500	14.333±0.559 <sup>a</sup>	11.741±0.971 <sup>a</sup>	15.296±0.329 <sup>a</sup>	27.630±1.157 <sup>a</sup>
<i>p</i> -value	<.0001	0.0002	<.0001	<.0001

<sup>a,b,c,d</sup> Means in the same column with different superscript letter following them are significantly different ( $p < 0.05$ ).

**Table (6)** regression coefficient of inhibition zone diameter (mm) of fungi on the different levels from methanolic clove extract

Clove levels	<i>A. niger</i>	<i>A. terreus</i>	<i>A. flavus</i>	<i>Curvularia. spp</i>
<i>a</i>	4.2317±0.516	4.3116±0.847	4.8141±1.062	8.1174±1.289
<i>b</i> -reg	0.1087±0.008	0.0884±0.013	0.1195±0.017	0.2008±0.021
<i>R</i> <sup>2</sup>	97.00	90.00	91.00	95.00
<i>p</i> -value	<.0001	<.0001	<.0001	<.0001

*a*: intercept; *b*-reg: regression coefficient; *R*<sup>2</sup>: coefficient of determination

### 3.8. Color change of clove and garlic extract applied on sandstone (CIE-lab Commission International d'Eclairage)

The aqueous garlic extract and the methanolic clove extract were applied after decolorization to cubes of sandstone in order to measure the color change on the surface of the sandstone compared to a standard sample, tab. (7). The aqueous garlic extract is excluded, and the clove extract is applied after removing its color on the sandstone sample.

**Table (7)** the color change of sandstone samples treated with methanolic clove extract and aqueous garlic extract compared to a control sample.

NO	Plant extract	ΔE
1	Methanolic Clove extract	1.77
2	Aqueous Garlic extract	2.85

### 3.9. Identified of the bioactive compounds present in the methanolic clove extract by using GC-MS.

Three antifungal compounds were found in the effective extract, according to the characterization of its constituent parts, tab. (8). & fig. (12). The majority of the compounds found in the current identification had antifungal activity. The GC-MC analysis detected the chemical composition of methanolic clove extract fig. (13) Mass spectroscopy of antifungal substance compound extract from clove and these results indicated that the substance under investigation showed: Bis Eugenol (Phenol, 2-Methoxy-4-(2-Propenyl) ( $C_{10}H_{12}O_2$ ) with MWt 164 (54.02%), Caryophyllene (Bicyclo [7.2.0] Undec-4-Ene,4,11,11-Trimethyl-8-Methylene-, [1R-(1R\*, 4E,9S\*)] ( $C_{15}H_{24}$ ) with MWt 204 (13.31%), Phenol (2-methoxy-4-(2-propenyl)- acetate) ( $C_{12}H_{14}O_3$ ) with MWt 206 (20.12%).

**Table (8)** GC-MS analysis of methanolic clove extract

Peak	RT	Name	Formula	Area	Area Sum%
1	12.68	Eugenol	$C_{10}H_{12}O_2$	54.02	7505976046.15
2	14.60	Caryophyllene	$C_{15}H_{24}$	13.31	1849699094.64
3	16.48	Phenol, 2-methoxy-4-(2-propenyl)-, acetate	$C_{12}H_{14}O_3$	20.12	2796177347.21
4	16.48	Eugenol	$C_{10}H_{12}O_2$	20.12	2796177347.21

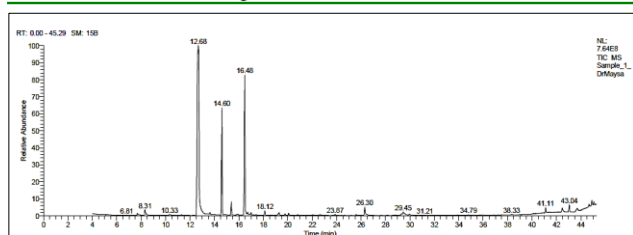


**Figure (12)** GC-MS of clove methanolic extract

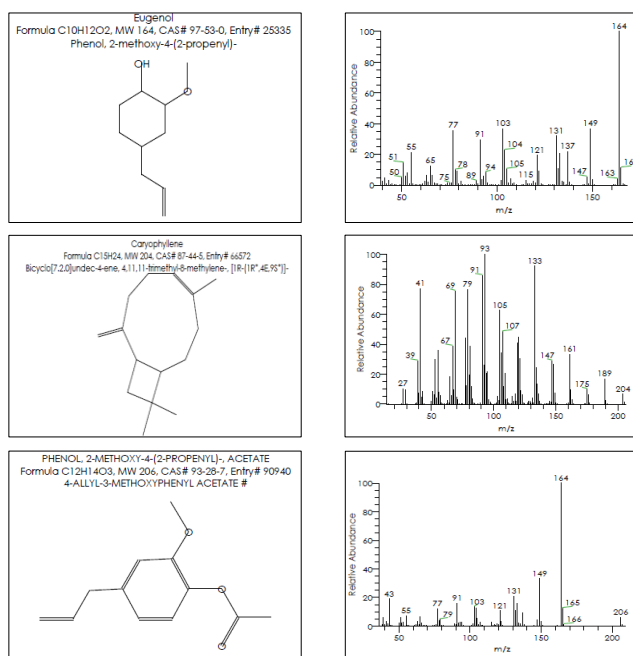


**Figure (13)** dimensional structures of active compound on Methanolic clove extract

## 4. Discussion

Most sandstone-isolated fungi in open area are well-adapted and grow in low-nutrient conditions. Fungi can fix the carbon from polluted air on the surface of sand stone as a source of nutrients, in addition to some elements found between quartz and some elements from bird waste and plants. This is to provide a source of organic carbon they need to grow, which is essential for their survival [11,39]. The acids produced by fungi on different types of rocks dissolve mineral elements, such as silicates, carbonates, phosphates, oxides, and other compounds, which are essentially while microbial geochemical cycles do by fungi. This is called biological weathering [40]. Among the damage consequences of fungal penetration of stones, which leads to fissures, and biochemical acidic metabolites, which cause the dissolving of stone minerals and oxidation of minerals, especially iron and manganese. Additionally, produce melanin, causing the discoloration of stone surface [19,29,41]. Genera of *Fusarium poae* and *Penicillium chrysogenum* were observed on stones at moderate incidence, where the most common fungus on stones is the genus *Apergillus* [42], and the *Apergillus. spp* and *curvularia. spp* cause biodeterioration on sand stone [6]. According to PLM and SEM, the sandstone has been altered feldspar to kaolinite [6,43], SEM-EDAX and mechanical characterization of sandstone cubes before and after infection from a simulation experiment showed extensive colonization of fungal hyphae around stone grains, which led to deterioration and loss of some mineral components present in the sandstone, moreover the hyphae penetrate minerals and dissolve them [44]. EDX of weathered sandstone surface showed the presence of some elements such as Si, O, Ca, C, Mg, Al, Si, K, Ti, and Fe with a high percentage. These results were reported as an indicator of deterioration. Examining *Curvularia. spp* growth on sand stone make black colonies under SEM, unbranched conidiophores, brown conidia, 3-septate, obovoidal. The conidia were fusiform with straight to slightly curve in shape [45], *A. terreus* colonies are brown color with a yellow to deep brown. pyriform vesicles, conidial heads [46], *A. flavus* conidiophore is a thick-walled branch, conidiophores are unbranched and are composed of the foot cell, stipe, and vesicle. Conidial heads light to deep yellow green, or green. colonies are granular, flat, Conidia are globose to sub globose [47], *A. niger* has black spore (conidia) due to its high melanin content, hyphae of *A. niger* are septate, hyaline and the conidiophores are long, becoming darker at the apex and ending in a globose to sub globose vesicle, tending to split into several loose columns with age [48,49]. According to XRD analysis, the sandstone consists mainly of silica (Qz), XRF analysis confirmed that the sandstone consists of a large percentage of silica in addition to some other elements such as aluminum (Al), calcium (Ca), iron (Fe), and potassium (K), magnesium (Mg), manganese (Mn), sodium (Na), Phosphorus (P), silicon (Si) and titanium (Ti) [50]. Some natural plant extracts showed great antimicrobial inhibitory effects against deteriorated fungal activity, such as clove, garlic, onion, cinnamon, rosemary and lemon grass [51]. Methanolic clove extract has antifungal activity because it contains active

compounds that inhibit fungi [52]. Aqueous garlic extract has antifungal activity [53]. GC-MS indicates the presence of the compounds Eugenol and Phenol, 2-methoxy-4-(2-propenyl) acetate [54]. Eugenol was the most active structure against fungal growth [55,56]. Moreover, the main compounds of clove extract are eugenol and  $\beta$ -caryophyllene, which are powerful antifungal agents [57].

## 5. Conclusion

The results in this study indicate the significant damage caused by fungal growth on the surface of sandstone located in an open area and its aesthetical appearance. It was necessary to inhibit fungal growth on sandstone by using plant extracts that have great effectiveness. Moreover, they are not harmful in the long time, whether for the effect on stone or the restorer. Tests and analyzes using the techniques mentioned above has been proven the damage caused by fungi on the surface of sandstone, including cracks, fissures, dissolving, and loss of some mineral elements. The above-mentioned scientific experiments also confirmed the effectiveness of methanolic clove extract after removing its color with activated charcoal in inhibiting fungal growth and preserving the aesthetic appearance of sandstone.

## References

- [1] Ullmann, T., Lange-Athinodorou, E., Göbel, A., et al. (2019). Preliminary results on the paleo-landscape of Tell Basta/Bubastis (eastern Nile delta): An integrated approach combining GIS-based spatial analysis, geophysical and archaeological investigations. *Quaternary Int.* 511:185-199.
- [2] Lange, E., Ullmann, T. & Baumhauer, R. (2016). Remote sensing the Nile delta: Spatio-temporal analysis of Bubastis/Tell Basta. *Ägypten und Levante/Egypt and the Levant.* 26: 377-392.
- [3] Pettijohn, F., Potter, P. & Siever, R. (1987). *Sand and sandstone*, 2<sup>nd</sup> ed. Springer Science & Business Media, LLC, NY.
- [4] Boggs, S. (2005), *Principles of sedimentology and stratigraphy*, 4<sup>th</sup> ed., Pearson, UK.
- [5] Liua, D., Sun, W., Ren, D. et al. (2019). Quartz cement origins and impact on storage performance in Permian Upper Shihezi Formation tight sandstone reservoirs in the northern Ordos Basin, China. *J. of Petroleum Science and Engineering.* 178: 485-496
- [6] El-Derby, A., Mansour, M. & Salem, M. (2016). Investigation the microbial deterioration of sandstone from the Osirian's sarcophagus chamber as affected by rising ground water level. *MAA* 16: 273-281
- [7] Winkler, E. (1987). Weathering and weathering rates of natural stone. *Environ. Geol. Water Sci.* 9: 85-92
- [8] Nord, A. & Tronner, K. (1995). Effect of acid rain on sandstone: The royal palace and the riddarholm church, Stockholm. *Water Air Soil Pollut* 85, 2719-2724
- [9] Ogburn, D., Sillar, B. & Sierra, J. (2013). Evaluating effects of chemical weathering and surface contamination on the in situ provenance analysis of building stones in the Cuzco region of Peru with portable XRF. *J. of Archaeological Science.* 40 (4): 1823-1837.
- [10] Warscheid, Th. & Braams, J. (2000). *Biodeterioration of stone: A review.* *Int. Biodeterioration & Biodegradation.* 46: 343-368.
- [11] Hirsch, P., Eckhardt, F. & Palmer, R. (1995). Methods for the study of rock-inhabiting microorganisms-A mini review. *J. of Microbiological Methods.* 23: 143-167.
- [12] Lan, W., Li, H., Wang, W., et al. (2010). Microbial community analysis of fresh and old microbial biofilms on Bayon temple sandstone of Angkor Thom, Cambodia. *Microb Ecol.* 60: 105-115.
- [13] Herrera, L., Arroyave, C., Guiamet, P., et al. (2004). Biodeterioration of peridotite and other constructional materials in a building of the Colombian cultural heritage. *Int. Biodeterioration & Biodegradation.* 54 (2-3): 135-141.
- [14] Sterflinger, K. & Piñar, G. (2013). Microbial deterioration of cultural heritage and works of art -- tilting at windmills?. *Appl Microbiol Biotechnol.* 97: 9637-9664.
- [15] Płaskowska, E., Patejuk, K., Lorenc, M. et al. (2023). Lichens and fungi on sandstone tombs at the historical Jewish cemetery in Wrocław (Poland), *Studies in Conservation.* 69 (1): 59-66.
- [16] Sazanova, K., Shchiparev, S. & Vlasov, D. (2014). Formation of organic acids by fungi isolated from the surface of stone monuments. *Microbiology.* 83: 516-522.
- [17] Farooq, M., Hassan, M. & Gul, F. (2015). Mycobial deterioration of stone monuments of Dharmarajika, Taxila. *J. of Microbiology & Experimentation.* 2 (1): 29-33.
- [18] Upton, D., Mason, M. & Wood, A. (2017). An accurate description of *Aspergillus niger* organic acid batch fermentation through dynamic metabolic modeling. *Biotechnology for Biofuels & Bioproducts.* 258 (2017), doi: 10.1186/s13068-017-0950-6 pp1-14.
- [19] Mohamed, S. & Ibrahim, S. (2018). Characterization and management of fungal deterioration of ancient limestone at different sites along Egypt, *Egyptian. J. Microbiol.* 53: 177-191.
- [20] Thomas, D., Perry, IV., Christopher, J. et al. (2005). Biodeterioration of stone. In: Arthur M. (ed.) *Scientific Examination of Art: Modern Techniques in Conservation and Analysis*, National Academies Press, USA, doi: 10.17226/11413.
- [21] Scheerer, S. (2008). *Microbial biodeterioration of outdoor stone monuments. Assessment methods and control strategies*, PhD, Cardiff Univ. UK.
- [22] De Carlo, E., Barresi, G. & Palla, F. (2022). Biodeterioration. In: Palla, F. & Barresi, G. (eds) *Biotechnology & Conservation of Cultural Heritage*, Springer Cham, Germany, pp. 1-30
- [23] Selvamohan, T., Ramadas, V. & Kishore, S. (2012). Antimicrobial activity of selected medicinal plants against some selected human pathogenic bacteria, *Advances in Applied Science Research.* 5: 3374-3381.
- [24] Wolverhampton, A., Abba, A., Isyaka, T., et al. (2012). Phytochemical characterization and antimicrobial studies on four folklore medicinal plants in semi-arid region of Borno State, Nigeria, *World J. of Advanced Research and Reviews.* 7 (1): 2581-9615
- [25] Azzouz, M. & Bullerman, L. (1982). Comparative antimycotic effects of selected herbs, spices, plant components and commercial antifungal agents, *J. of Food Protection.* 45 (14):1298-1301



- [26] Thombre, R., Shinde, V., Thaiparambil, E., et al. (2016). Antimicrobial activity and mechanism of inhibition of silver nanoparticles against extreme halophilic archaea, antimicrobials. *Frontiers in Microbiology*. 7, oi: 10.3389/fmicb.2016.01424.
- [27] Sakr, A., Ali, M., Ghaly, M., et al. (2012). Discoloration of ancient Egypt mural paintings by streptomyces strains and methods of its removal. *IJCS*. 3: 249-258.
- [28] Mohamed, E. (2022). Study correlation between physical-mineralogical properties of sandstone used in Ptolemaic temples in upper Egypt and its weathering resistance. *J. of Minerals and Materials Characterization and Engineering*. 10 (5): 371-384.
- [29] Milica, L. & Jelena, V. (2009). Role of fungi in biodegradation process of stone historic buildings. *Zbornik Matice Srpske za Prirodne Nauke*. 2009 (116). 245-251
- [30] Mansour, M. (2013). Proactive investigation using bio-agents and fungicide for preservation of Egyptian stone sarcophagus. *J. of Applied Sciences Research*. 9 (3). 1917-1930.
- [31] Sakr, A., Ali, M. & Ghali, M. (2013). The relationship between salts and growth of streptomyces colonies isolated from mural paintings in ancient Egyptian tomb, *Conservation Science in Culture Heritage*. 13 (1): 313-330.
- [32] Sasirekha, B., Megha, D., Chandra, M., et al. (2015), Study on effect of different plant extracts on microbial biofilms. *Asian J. of Biotechnology*. 7 (1): 1-12.
- [33] Purkait, M., Maiti, M., Gupta, S., et al. (2007). Removal of congo red using activated carbon and its regeneration. *J. of Hazardous Materials*. 145 (1-2): 287-295.
- [34] Tippayawat, P., Phromviyo, N., Boueroy, P., et al. (2016). Green synthesis of silver nanoparticles in aloe vera plant extract prepared by a hydrothermal method and their synergistic antibacterial activity. *Peer J*. 4, doi:10.7717/peerj.2589
- [35] Lopez, C., Nitisinprasert, S., Wanchaitanawong, P., et al. (2003). Antimicrobial activity of medicinal plant extracts against foodborne spoilage and pathogenic microorganisms. *Kasetsart J. (Nat. Sci.)*. 37. 460-467.
- [36] Humphries, R., Ambler, J., Mitchell, S., et al. (2018). CLSI methods development and standardization working group best practices for evaluation of antimicrobial susceptibility tests. *J. of Clinical Microbiology*. 56 (4), 10.1128/jcm.01934-17.
- [37] Yassin, M., Mostafa, A. & Al-Askar, A. (2020), In vitro anticandidal potency of *Syzygium aromaticum* (clove) extracts against vaginal candidiasis, *BMC Complementary Medicine & Therapies*. 20, doi: 1186/s12906-020-2818-8.
- [38] Abd El-Kareem, M., Rabbih, M., Silem, E., et al. (2016), Application of GC/EIMS in combination with semi-empirical calculations for identification and investigation of some volatile components in basil essential oil. *Int. J. of Analytical Mass Spectrometry and Chromatography*. 4 (1): 14-25.
- [39] Suihko, M., Alakomi, H., Gorbushina, A., et al. (2007). Characterization of aerobic bacterial and fungal microbiota on surfaces of historic Scottish monuments. *Systematic and Applied Microbiology*. 30: 494-508
- [40] Torre, M., Gomez-Alarcon, G., Melgarejo, P., et al. (1991). Fungi in weathered sandstone from Salamanca cathedral, Spain. *STOTEN*. 107: 159-168
- [41] Harley, A. & Gilkes, R. (2000), Factors influencing the release of plant nutrient elements from silicate rock powders: A geochemical overview. *Nutr Cycl Agroecosyst*. 56: 11-36.
- [42] Maghazy, S., Abdel-Zaher, H. & EL-gendidy, Z. (2012), Indoor aeromycobiota of monumental sites in Minia Governorate. *J. of Basic & Applied Mycology*. 3: 49-59.
- [43] Nagtegaal, P. (1978). Sandstone-framework instability as a function of burial diagenesis, *J. of the Geological Society*. 135 (1): 101-105.
- [44] Jain, A. Bhadauria, S., Kumar, V., et al. (2009). Biodegradation of sandstone under the influence of different humidity levels in laboratory conditions. *Building and Environment*. 44: 1276-1284
- [45] Kusai, N., Azmy, M., Zulkifly, S., et al. (2016), Morphological and molecular characterization of curvularia and related species associated with leaf spot disease of rice in Peninsular Malaysia, *Rend. Fis. Acc. Lincei*. 27: 205-214.
- [46] Zulkifli, N. & Zakaria, L. (2017). Morphological and molecular diversity of aspergillus from corn grain used as livestock feed. *HAYATI J. of Biosciences*. 24: 26-34.
- [47] Gourama, H. & Bullerman, L. (1995). *Aspergillus flavus* and *Aspergillus parasiticus*: Aflatoxigenic fungi of concern in foods and feeds: A review. *J. of Food Protection*. 58 (12): 1395-1404.
- [48] Paul, S., Ludeña, Y., Villena, G., et al. (2017). High-quality draft genome sequence of a biofilm forming lignocellulolytic *Aspergillus niger* strain ATCC 10864. *Standards in Genomic Sciences*. 12 (37), doi: 10.1186/s40793-017-0254-2
- [49] Romsdahl, J., Blachowicz, A., Chiang, A., et al. (2018). Characterization of *aspergillus niger* isolated from the international space station. *mSystems*. 3 (5), doi: 10.1128/mSystems.00112-18
- [50] El-Gohary, M. (2013). Evaluation of treated and untreated Nubia Sandstone using ultrasonic as a non-destructive technique. *J. of Archaeological Science*. 40, (4): 2190-2195
- [51] Ceylan, E. & Fung, D. (2004), Antimicrobial activity of spices. *J. of Rapid Methods and Automation in Microbiology*. 12 (1), doi:10.1111/j.1745-4581.2004.tb00046.x
- [52] Mekky, A., Emam, A., Selim, M., et al. (2023), Antibacterial and antineoplastic MCF-7 and HePG-2 characteristics of the methanolic (80%) clove (*Syzygium aromaticum* L.) extract. *Biomass Conversion and Biorefinery*. 14: 16787-16798
- [53] Hayat, S., Cheng, Z., Ahmad, H., et al. (2016), Cultivars; allicin containing aqueous garlic extracts trigger antioxidants in cucumber. *Frontiers in Plant Science*. 7, doi: 10.3389/fpls.2016.01235.
- [54] Moralesa, M., Villarrea, A., Marcelino, L., et al. (2022), Chemical composition and antifungal and nematocidal activities of the hexanic and methanolic extracts of *Syzygium aromaticum*, Research article. *ScienceAsia*. 49 (1), doi: 10.2306/scienceasia1513-1874.2022.143.

- [55] Reddy, C., Reddy, K., Prameela, M., et al. (2007). Identification of antifungal component in clove that inhibits *Aspergillus* spp. colonizing rice grains, *J. Mycology & Plant Pathology*. 37 (1): 87-94.
- [56] Carrasco, H., Raimondi, M., Svetaz, L., et al. (2012), Antifungal activity of eugenol analogues. influence of different substituents and studies on mechanism of action. *Molecules*. 17: 1002-1024
- [57] Hiwandika, N., Sudrajat, S. & Rahayu, I. (2021). Antibacterial and antifungal activity of clove extract (*Syzygium aromaticum*): Review, *Eureka Herba Indonesia*. 2 (2): 93-103.